Synergistic Inhibitory Effect of Polymyxin B in Combination with Ceftazidime against Robust Biofilm Formed by *Acinetobacter baumannii* with Genetic Deficiency in AbaI/AbaR Quorum Sensing

Yinyue Li,[a] Bo Wang,[b] Feng Lu,[a,d] Juhee Ahn,[c] Wenwen Zhang,[a] Liangliang Cai,[a] Jiahui Xu,[a] Yi Yin,[a] Qingchao Cao,[a] Zhenyu Ren,[a] Xinlong He[a,d,e,f]

[a]Department of Pathogen Biology, School of Medicine, Yangzhou University, Yangzhou, People's Republic of China
[b]Department of Clinical Laboratory, First Affiliated Hospital of Anhui Medical University, Hefei, Anhui, People's Republic of China
[c]Department of Medical Biomaterials Engineering, College of Biomedical Science, Kangwon National University, Chuncheon, Gangwon, South Korea
[d]Jiangsu Key Laboratory of Experimental and Translational Non-coding RNA Research, Yangzhou University, Yangzhou, People's Republic of China
[e]Jiangsu Key Laboratory of Zoonosis, Yangzhou University, Yangzhou, People's Republic of China
[f]Jiangsu Co-Innovation Center for the Prevention and Control of Important Animal Infectious Diseases and Zoonosis, College of Veterinary Medicine, Yangzhou University, Yangzhou, People's Republic of China

Yinyue Li and Bo Wang contributed equally to this article. Author order was determined randomly.

ABSTRACT Carbapenem resistance of *Acinetobacter baumannii* poses challenges to public health. Biofilm contributes to the persistence of *A. baumannii* cells. This study was designed to investigate the genetic relationships among carbapenem resistance, polymyxin resistance, multidrug resistance, biofilm formation, and surface-associated motility and evaluate the antibiofilm effect of polymyxin in combination with other antibiotics. A total of 103 clinical *A. baumannii* strains were used to determine antibiotic susceptibility, biofilm formation capacity, and motility. Enterobacterial repetitive inter-genic consensus (ERIC)-PCR fingerprinting was used to determine the genetic variation among strains. The distribution of 17 genes related to the resistance-nodulation-cell division (RND)-type efflux, autoinducer-receptor (AbaI/AbaR) quorum sensing, oxacillinases (OXA)-23, and insertion sequence of IS*Aba1* element was investigated. The representative strains were chosen to evaluate the gene transcription and the antibiofilm activity by polymyxin B (PB) in combination with merapenem, levofloxacin, and ceftazidime, respectively. ERIC-PCR-dependent fingerprints were found to be associated with carbapenem resistance and multidrug resistance. The presence of bla_{OXA-23} was found to correlate with genes involved in IS*Aba1* insertion, AbaI/AbaR quorum sensing, and AdeABC efflux. Carbapenem resistance was observed to be negatively correlated with biofilm formation and positively correlated with motility. PB in combination with ceftazidime displayed a synergistic antibiofilm effect against robust biofilm formed by an *A. baumannii* strain with deficiency in AbaI/AbaR quorum sensing. Our results not only clarify the genetic correlation among carbapenem resistance, biofilm formation, and pathogenicity in a certain level but also provide a theoretical basis for clinical applications of polymyxin-based combination of antibiotics in antibiofilm therapy.

IMPORTANCE Deeper explorations of molecular correlation among antibiotic resistance, biofilm formation, and pathogenicity could provide novel insights that would facilitate the development of therapeutics and prevention against *A. baumannii* biofilm-related infections. The major finding that polymyxin B in combination with ceftazidime displayed a synergistic antibiofilm effect against robust biofilm formed by an *A. baumannii* strain with genetic deficiency in AbaI/AbaR quorum sensing further

provides a theoretical basis for clinical applications of antibiotics in combination with quorum quenching in antibiofilm therapy.

KEYWORDS *Acinetobacter baumannii*, carbapenem resistance, polymyxin B, antibiofilm formation, quorum sensing

*A*cinetobacter baumannii is an important opportunistic pathogen causing various nosocomial infections, including skin and soft tissue infections (1), urinary tract infections (2), pneumonia (3), and even bacteremia (4). With the extensive use and especially the abuse of antibiotics, resistant bacteria emerged quickly, and multidrug-resistant (MDR) (5) *A. baumannii* has become widespread. Carbapenem antibiotics with broad antibacterial spectrum and high bactericidal activity are the first line of treatment for severe infections caused by MDR *A. baumannii*. However, carbapenem-resistant *A. baumannii* (CRAB) has become one of the most common nosocomial pathogens, especially in the intensive care unit (ICU) (6–8). The frequent emergence of CRAB, especially those with high virulence, poses severe challenges to public health (9, 10). The interplay between genetic virulence regulation and carbapenem resistance seems to be strain dependent (11). Molecular typing plays a key role in understanding the basic mechanism of *A. baumannii* infection and discovering the relationship between bacterial species (12).

A. baumannii resistance to carbapenems is more closely related to the production of oxacillinase (OXA)-type carbapenemases (13). Among these D class β-lactamases, OXA-23 is the most common carbapenemase produced by CRAB in recent years (14). The insertion element IS*Aba1* is essential for high-level production of OXA-23 (15). The widely distributed resistance-nodulation-cell division (RND) family efflux pumps, including AdeABC, AdeIJK, and AdeFGH, are also important factors that have to be considered for carbapenem resistance in *A. baumannii* (16). In addition, the biofilm-forming capacity of *A. baumannii* has been thought to play an essential role in the persistence of *A. baumannii* cells under severe environmental conditions (17). Surface-associated motility of *A. baumannii* is likely to be mediated by type IV pili, an important virulence factor involved in bacterial pathogenicity (18). Similar to the typical LuxI/LuxR (19), AbaI/AbaR quorum sensing plays an important role in maintaining the expression of bla_{OXA-51} and *ampC* resistance genes, as well as the carbapenem resistance phenotypes in *A. baumannii* (20). The AbaI/AbaR system is also required for the regulation of biofilm formation and motility (21). However, the genetic relationships among carbapenem resistance, MDR, quorum sensing, biofilm formation, and motility remain unclear.

At the time when carbapenem resistance was widespread, polymyxins were particularly important as the last line of defense in the treatment of multidrug-resistant bacterial infections. Low-dose administration of meropenem, levofloxacin, and tigecycline displays increased risk of biofilm-associated infections (22, 23). Although polymyxin in combination with these conventional antibiotics has partially shown a pleasing synergistic inhibitory effect on the proliferation of *A. baumannii* cells (24), its effect on biofilm formation is still unclear. This study was designed to investigate the genetic correlation among carbapenem resistance, polymyxin resistance, MDR, AbaI/AbaR quorum sensing, motility, and biofilm formation and evaluate the potential antibiofilm effect of polymyxin in combination with meropenem, levofloxacin, and ceftazidime against *A. baumannii*.

RESULTS AND DISCUSSION

ERIC-PCR-dependent fingerprints of *A. baumannii* are associated with carbapenem resistance and multidrug resistance. According to Clinical and Laboratory Standards Institute (CLSI), the minimum inhibitory concentration (MIC) is visually defined as the absence of growth in cation-adjusted Mueller-Hinton (MH) medium. In this study, we found that there was no significant difference between the MIC values obtained by using MH and nutrient broth (NB) media and for antibiotics of meropenem (MEM), levofloxacin (LEV),

ceftazidime (CAZ), and polymyxin B (PB), respectively. Enterobacterial repetitive intergenic consensus (ERIC)-PCR fingerprinting has been demonstrated to be a reliable technique for discriminating intraspecific variations (25). Using ERIC-PCR analysis, a total of 103 *A. baumannii* strains were classified into nine ERIC-PCR-dependent genotypes showing four groups (a group contains more than three strains) with types of II ($n = 53$, 51.5%), III ($n = 20$, 19.4%), IV ($n = 11$, 10.7%), and V ($n = 13$, 12.6%); two strains with type of I; and four single strains with type of VI, VII, VIII, and IX, respectively (Fig. S1). The bacterial sources mostly came from sputum ($n = 70$, 68%) followed by wounds ($n = 19$, 18.5%) (Fig. S2). Among sputum and wound-derived strains, carbapenem-resistant strains accounted for 72.9 and 78.9%, respectively, which remained at the same level as the 75.1% resistance rate of the previous year (26). This observation suggests that respiratory tract infections and wound infections caused by CRAB are still burdens for health care in China. The type II and III strains were observed to be dominated by carbapenem-resistant strains (Fig. 1), showing 96.2 and 95% resistance rates (Table 1), respectively, while the IV and V type strains were mainly carbapenem-sensitive strains (72.7 and 84.6%). These observations suggest that the carbapenem resistance of *A. baumannii* is intrinsically related to specific genotypes. The ERIC-dependent fingerprints can be used as a useful genetic marker for the epidemiological investigation of carbapenem-resistant *A. baumannii*.

As shown in Fig. 1, most of the type II and III strains also displayed resistance to LEV and CAZ, and more than 70% of type II and III strains showed MDR to MEM, LEV, and CAZ (Table 1). PB is used as the last-line drug for the treatment of multidrug-resistant bacterial infections. A recent meta-analysis has shown that the overall frequency of polymyxin-resistant *A. baumannii* in hospitals worldwide is 13%, and the average incidence of infections by polymyxin-resistant *A. baumannii* in hospitalized patients from 2012 to 2017 in Eastern Asian countries, including China, is 18% (27). As shown in Table 1, there was no genotype difference in the distribution of PB-resistant strains. In mechanism, resistance to carbapenems, quinolones, and cephalosporins in *A. baumannii* is primarily mediated by mobile genetic elements (28). Plasmids that carry resistance genes present in this bacterium usually carry genes that encode low susceptibility to more than one class of antibiotics (29). Resistance to polymyxins in *A. baumannii* is basically mediated by chromosomal mutations (30), which hardly correlate with resistance to other antibiotics. Despite the advancement of *mcr* as a gene encoding plasmid-mediated resistance to polymyxins in nonfermenting Gram-negatives such as *A. baumannii*, it still represents a limited mechanism in this group of pathogens compared to chromosomal mutations in the *pmrCAB* and *lpxACD* operons (30). It should be noted that the PB resistance rate (41.8% in average) was much higher than the world average in recent years. In addition, the multidrug-resistant CRAB that was resistant to PB appeared in different genotypes, and its proportion in type II strains was even as high as 26% (Table 1). Therefore, the development of antibiotic resistance of *A. baumannii* in China is not a positive sign. From the perspective of effective treatment of MDR *A. baumannii* infections and curbing the development of antibiotic resistance, our observations stress the urgency of new drug development and the importance of current polymyxin combination therapy.

The presence of *bla*$_{OXA-23}$ is genetically correlated with IS*Aba1* insertion, AbaI/AbaR quorum sensing, and AdeABC efflux. In this study, 85.3% of MEM-resistant and 100% of MEM-intermediate *A. baumannii* strains were observed to harbor *bla*$_{OXA-23}$ gene (Fig. 1). The *bla*$_{OXA-23}$ gene was detected in more than 85% of type II and III strains (Table 2), which is consistent with the carbapenem-resistance phenotype. All *bla*$_{OXA-23}$-harboring *A. baumannii* strains were also observed to contain IS*Aba1* element (Fig. 1). Data analysis also showed a positive correlation in gene presence between *bla*$_{OXA-23}$ and IS*Aba1* (Table 3), suggesting a genetic correlation between *bla*$_{OXA-23}$ and IS*Aba1*. The IS*Aba1* element is commonly upstream of the *bla*$_{OXA-23}$ (31), which forms a neighbor relation in genome structure that is crucial for both the horizontal transfer of *bla*$_{OXA-23}$ (32) and the vertical inheritance of IS*Aba1*. Quorum sensing has been proven to be important for success of an intraspecific conjugation of *Agrobacterium* (33) and an interspecific conjugation between *Escherichia coli* and *Pseudomonas aeruginosa*
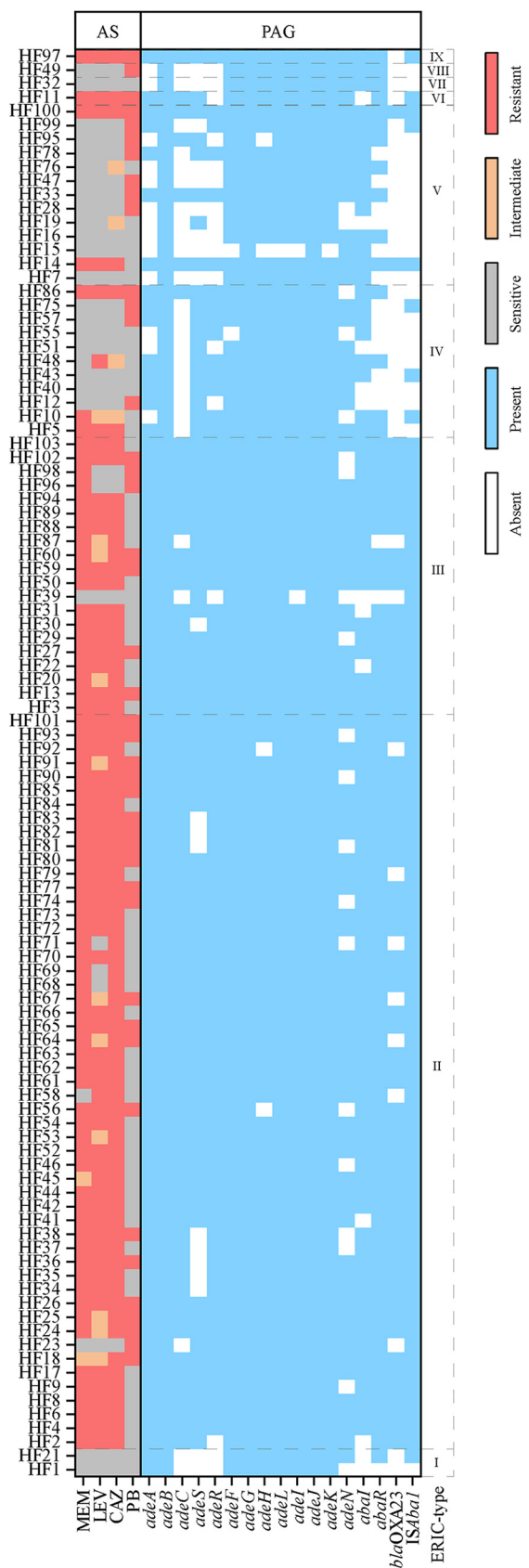
FIG 1 Heat map of antibiotic resistance and gene presence in *Acinetobacter baumannii* strains. The roman numerals on the right (I to IX) indicate the different clades identified from the ERIC-PCR-

(34). On account of a correlated presence of bla_{OXA-23} and *abaR* (Table 3), AbaI/AbaR quorum sensing might also be associated with the horizontal transfer of bla_{OXA-23}. OXA genes are widespread in clinic *A. baumanii*; most of them are bla_{OXA-23} and bla_{OXA-51} (35). IS*Aba1* insertion could contribute to high-level expression of bla_{OXA-51}, as well as bla_{OXA-23} (36). The lack of consideration of bla_{OXA-51} is a limitation of this study.

Overexpression of RND family efflux systems is generally considered to play a major role in the MDR of *A. baumannii* (37). Except for *adeB* and *adeG*, all other genes of RND-type efflux systems were found to have different degrees of deficiency in type II to V strains (Fig. 1), and the missing rate of *adeC* was found to be even higher than 90% in IV type strains (Table 2). Strains with a complete efflux system accounted for more than 80% of type II and type III strains, and the distribution of AdeFGH in type III strains even reached 100% (Table 2). The completeness of these efflux systems in IV and V strains was relatively low, and the AdeABC efflux system was the most prominent, showing proportions of 9.1 and 23.1% in IV and V strains (Table 2). The significant difference in the distribution of the AdeABC system in the type II, III, IV, and V strains is likely to be the main reason for the significant difference in the distribution of multidrug resistance in different genotype strains in this study. The bla_{OXA-23} was found to coexist with genes related to AdeABC efflux system, showing correlation coefficient as high as 0.796 ($P < 0.01$) (Table 3). The expression of bla_{OXA-23} was also observed to correlate with both *adeB* and *adeJ* at an mRNA level (Fig. 2B). These observations provide a reasonable explanation for the phenomenon that CRAB strains commonly exhibit the MDR phenotype (38). IS*Aba1* element is thought to contribute to the carbapenem resistance by affecting not only the expression of β-lactamases but also the regulation of RND-type efflux (15, 39). The expression of *adeABC* has been reported to be regulated by a two-component signaling system encoded by *adeR* and *adeS* (40), while the expression of *adeFGH* and *adeIJK* is regulated by *adeL* (41) and *adeN* (42), respectively. Mutation in *adeS* by IS*Aba1* insertion is associated with an increased expression of AdeABC, as well as a decreased susceptibility to tigecycline in *Acinetobacter* spp. (39, 43). An insertion of IS*Aba1* in *adeN* has been previously reported (44), which might have led to diminished susceptibility to antibiotics that are substrates for the AdeIJK. In this study, structurally, 40.3% of MDR *A. baumannii* strains were found to harbor *adeN* with an insertion of IS*Aba1* ($adeN^{\wedge IS Aba1}$) at a locus between 298 and 299 (Fig. S3). A correlated presence of IS*Aba1* with *adeS*, *adeR*, and *adeL* (Table 2) might increase the risk of overexpression of these RND-type efflux systems, resulting in MDR.

Carbapenem resistance is negatively correlated with biofilm formation and positively correlated with motility. The ability to form biofilms is closely related to the persistence of bacteria in unfavorable environments and is considered the main cause of chronic infections (45). Motility has been linked to increased pathogenicity in various bacteria, including *A. baumannii* (46, 47). Reduced fitness and virulence have been demonstrated to be associated with increased resistance to certain antibiotics, including polymyxins (11, 48) and ciprofloxacin (49). There were no significant differences in biofilm and motility among strains of different genotypes (II to V) (data not shown). However, in general, as shown in Table 3, both the carbapenem-resistant phenotype and the presence of bla_{OXA23} were significantly negatively correlated with the formation of biofilms ($P < 0.01$), and the presence of bla_{OXA-23} that was negatively correlated with the biofilm formation was positively correlated with motility ($P < 0.05$). An inverse correlation between motility and biofilm formation provides important information for the choice of antimicrobial and antibiofilm therapy of infections. In this study, the presence of IS*Aba1* that was negatively correlated with the biofilm formation was also found to be positively correlated with the motility (Table 3). Mutation in *fpvA* (a TonB re-

FIG 1 Legend (Continued)
dependent fingerprints. Breakpoints were defined for ceftazidime as ≤ 8, 16, and ≥ 32 μg/mL; for levofloxacin as ≤ 2, 4, and ≥ 8 μg/mL; for meropenem as ≤ 4, 8, and ≤ 16 μg/mL; and for polymyxin B as ≤ 2 and ≥ 4 μg/mL for designating strains as antibiotic sensitive, intermediate (if available), and resistant, respectively. AS, antibiotic susceptibility; PAG, presence or absence of gene detected; MEM, meropenem; LEV, levofloxacin; CAZ, ceftazidime; PB, polymyxin B.

TABLE 1 Proportion of antibiotic-resistant *A. baumannii* strains[a]

	Proportion of antibiotic-resistant strains (%)			
Antibiotic	ERIC type II	ERIC type III	ERIC type IV	ERIC type V
MEM	92.5	95	27.3	15.4
LEV	79.2	70	27.3	15.4
CAZ	98.1	85	18.2	15.4
PB	41.5	35	36.4	53.8
Multidrug				
MEM, LEV, CAZ	75.5	70	18.2	15.4
PB, MEM, LEV, CAZ	26.4	20	9.1	7.7

[a]MEM, meropenem; LEV, levofloxacin; CAZ, ceftazidime; PB, polymyxin B.

ceptor homologue) has been demonstrated to be associated with an accelerated motility and a decreased production of extracellular polysaccharides and quorum-sensing molecules in *Pseudomonas syringae* (50). Thus, a disruption of TonB-dependent siderophore receptor gene that can be caused by IS*Aba1* insertion (44) could be involved in an upregulation of motility and a concurrent downregulation of biofilm formation observed in this study. This study also establishes a link between IS*Aba1* and AbaI/AbaR quorum sensing on account of a correlated presence of IS*Aba1* and *abaR*. However, the inner connection between IS*Aba1* and AbaI/AbaR needs to be further clarified.

Synergistic antimicrobial effects of PB in combination with antibiotics against *A. baumannii*. Since the return of polymyxins as effective drugs for the treatment of multidrug-resistant bacterial infections, especially carbapenem-resistant Gram-negative bacterial infections, the emergence of PB-resistant *A. baumannii* has increased in recent years (51, 52). In this study, the antimicrobial effect of PB in combination with

TABLE 2 Proportion of *A. baumannii* strains with the presence of genes

	Proportion of *A. baumannii* strains with genes (%)			
Gene	ERIC type II	ERIC type III	ERIC type IV	ERIC type V
Carbapenemases				
bla$_{OXA23}$	86.8	90	0	15.4
Insertion sequence				
IS*Aba1*	100	100	27.3	23.1
AdeABC system				
adeA	100	100	72.7	38.5
adeB	100	100	100	100
adeC	98.1	90	9.1	30.8
adeS	84.9	95	100	46.2
adeR	98.1	95	81.8	38.5
adeA, adeB, adeC, adeS, adeR	83	85	9.1	23.1
AdeFGH system				
adeF	100	100	90.9	92.3
adeG	100	100	100	100
adeH	96.2	100	100	84.6
adeL	100	100	100	92.3
adeF, adeG, adeH, adeL	96.2	100	90.9	84.6
AdeIJK system				
adeI	100	95	100	92.3
adeJ	100	95	100	100
adeK	100	95	100	92.3
adeN	81.1	80	72.7	84.6
adeI, adeJ, adeK, adeN	81.1	80	72.7	76.9
Quorum sensing				
abaI	96.2	85	72.7	92.3
abaR	100	90	36.4	53.8
abaI, abaR	96.2	80	36.4	53.8

TABLE 3 Correlation matrix of Spearman correlation coefficients between gene presence, antibiotic resistance, biofilm formation, and motility in *A. baumannii*

Factor	Efflux systems										Quorum sensing		Antibiotic resistance				Biofilm	Motility
	bla_{OXA-23}	ISAba1	adeA/B/C	adeS	adeR	adeF/G/H	adeL	adeI/J/K	adeN	adeN^ISAba1	abaI	abaR	MEM	LEV	CAZ	PB		
bla_{OXA-23}	1	0.676[a]	0.796[a]	0.195[b]	0.539[a]	0.208[b]	0.132	0.188	0.042	0.403[a]	0.233[b]	0.573[a]	0.746[a]	0.656[a]	0.717[a]	−0.023	−0.418[a]	0.219[b]
ISAba1		1	0.739[a]	0.300[a]	0.619[a]	0.222[b]	0.196[b]	0.103	0.056	0.332[a]	0.192	0.581[a]	0.737[a]	0.568a	0.711[a]	−0.011	−0.348[a]	0.085
Efflux systems																		
adeA/B/C			1	0.321[a]	0.627[a]	0.174	0.166	0.236[b]	0.042	0.391[a]	0.265[a]	0.719[a]	0.847[a]	0.726[a]	0.865[a]	0.057	−0.503[a]	0.241[b]
adeS				1	0.443[a]	0.003	0.202[b]	0.109	0.069	0.269[a]	−0.025	0.128	0.318[a]	0.217[b]	0.314[a]	−0.032	−0.002	−0.049
adeR					1	0.143	0.223[b]	0.317[a]	0.046	0.235[b]	0.491[a]	0.459[a]	0.625[a]	0.524[a]	0.609[a]	0.058	−0.277[a]	0.105
adeF/G/H						1	0.438[a]	0.296[a]	0.118	0.148	−0.082	0.153	0.172	0.125	0.177	0.008	−0.058	0.105
adeL							1	0.704[a]	−0.049	0.065	−0.036	0.231[b]	0.166	0.142	0.17	0.084	−0.033	0.042
adeI/J/K								1	0.109	0.092	0.168	0.328[a]	0.236[b]	0.203[b]	0.241[b]	0.119	−0.14	0.143
adeN									1	0.322[a]	0.051	0.128	−0.019	0.034	0.071	−0.082	−0.12	0.007
adeN^ISAba1										1	0.04	0.281[b]	0.400[a]	0.325[a]	0.349[a]	−0.083	−0.200[b]	0.171
Quorum sensing																		
abaI											1	0.346[a]	0.263[a]	0.187	0.253[b]	0.185	−0.18	0.027
abaR												1	0.657[a]	0.596[a]	0.656[a]	0.037	−0.414[a]	0.270[a]
Antibiotic resistance																		
MEM													1	0.729[a]	0.876[a]	−0.012	−0.440[a]	0.177
LEV														1	0.824[a]	−0.107	−0.409[b]	0.219[b]
CAZ															1	−0.08	−0.459[a]	0.16
PB																1	−0.029	0.138
Biofilm																	1	−0.303[a]
Motility																		1

[a] The correlation was significant at a confidence level of 0.01 (two-tailed).
[b] The correlation was significant at a confidence level of 0.05 (two-tailed).
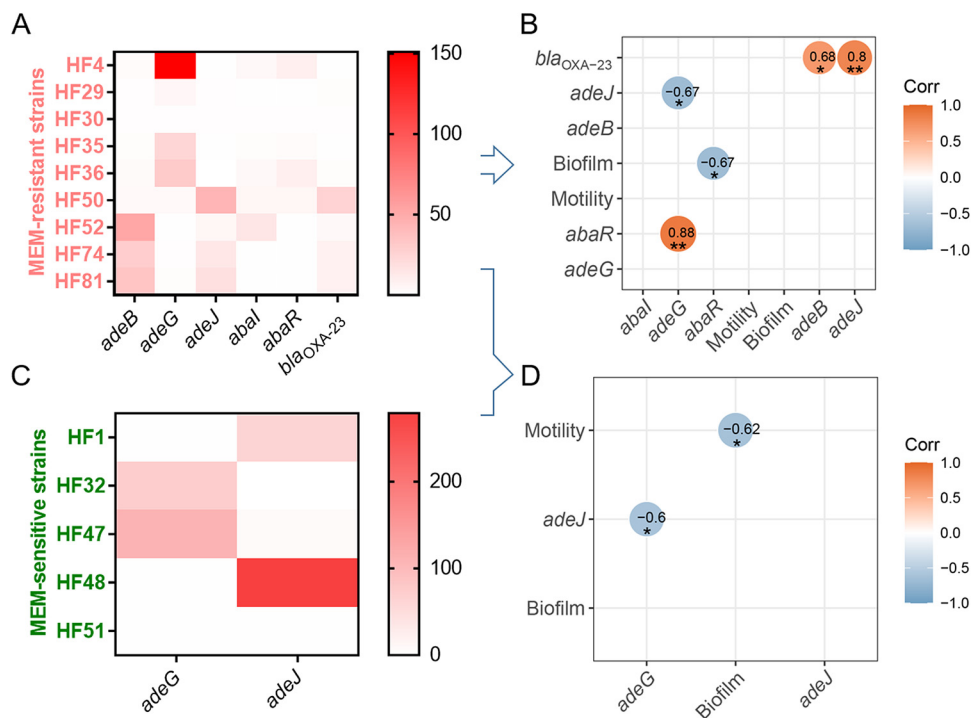
FIG 2 Gene expression in representative strains of *A. baumannii*. (A, C) Heat maps of gene expression in representative MEM-resistant (A) and MEM-sensitive strains (C). The data are presented as means of three biological replicates. (B) Matrix graph of correlation (Corr) among gene expression, biofilm formation, and motility in representative MEM-resistant strains. (D) Matrix graph of correlation among gene expression, biofilm formation, and motility in representative MEM-resistant strains and MEM-sensitive strains. Arrows indicate that the representative strains used for correlation analysis were derived from strains used for gene expression heat map analysis. *, significantly correlated at a *P* value of 0.05; **, significantly correlated at a *P* value of 0.01.

antibiotics on the growth of planktonic cells varied on the strains and genotypes. A synergistic inhibition effect on the growth of planktonic cells of *A. baumannii* strains was observed in the combination of PB and MEM against HF15 (V type) and the combination of PB and CAZ against HF51 (IV-type) (Fig. 3). The additivity effect was observed in the combination of PB and LEV against HF1, HF15, and HF32 and in the combination
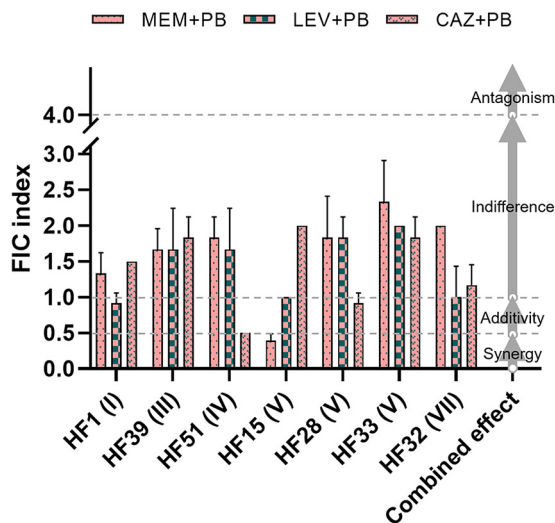

FIG 3 Fractional inhibitory concentration (FIC) index of polymyxin B in combination with meropenem (MEM), levofloxacin (LEV), and ceftazidime (CAZ) against representative strains of *A. baumannii*. The combined antimicrobial effect was interpreted as synergy (FIC index [FICI] $\leq$ 0.5), additivity (FICI > 0.5 and <1), indifference (FICI $\geq$ 1 and < 4), and antagonism (FICI $\geq$ 4). The data are presented as means $\pm$ standard deviation (SD) of three biological replicates.
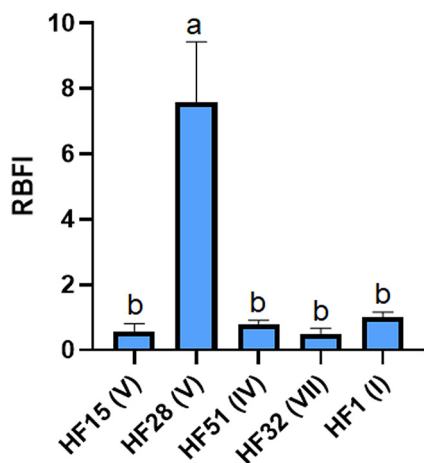
FIG 4 Relative biofilm formatin index (RBFI) of representative strains of *A. baumannii*. The roman numerals (I to IX) indicate the different clades of strains identified from the ERIC-PCR-dependent fingerprints. The data are presented as means ± SD of three biological replicates and the significances were determined by nonparametric one-way analysis of variance (ANOVA). Columns with different lowercase letters (a and b) within treatments are significantly different at $P < 0.05$.

of PB and CAZ against HF28 (Fig. 3). The other combinations showed an indifference effect with FICs between 1 and 4 (Fig. 3). This observation is consistent with earlier studies (53, 54), indicating that PB combination therapy is potentially more effective against *A. baumannii* infections compared with monotherapy with PB. Strains of HF15, HF28, HF51, HF32, and HF1 that show FIC ≤ 1 (Fig. 3 and Fig. S4) to antibiotic combinations were further chosen to assess the antibiofilm properties.

Robust biofilm is formed by an *A. baumannii* strain with genetic deficiency in AbaI/AbaR quorum sensing. More than a role in MDR, RND-type efflux systems have been increasingly proven to be essential for biofilm formation by many Gram-negative bacteria (55). AbaI has been proven to nonspecifically produce a variety of quorum sensing molecules of *N*-acyl homoserine lactones (AHLs), including 3-OH-C12-HSL (56), that are likely to be the substrates for the RND-type efflux pumps and competitively bind with AbaR, leading to different responses in biofilm formation and motility (57). In this study, instead, the native expression of *abaI* (correlation [Corr] = −0.45; $P > 0.05$) and *abaR* (Corr = −0.67; $P < 0.05$) were both observed to be negatively correlated with the biofilm formation (Table 3). Meanwhile, the native expression of *adeG* that was positively correlated with *abaR* was observed to be negatively correlated with the expression of *adeJ* (Corr = −0.67; $P < 0.05$) and *adeB* (Corr = −0.52; $P > 0.05$) (Table 3), likely showing an AdeFGH-dependent AbaI/AbaR quorum sensing. However, *A. baumannii* does not seem to tilt the weight of quorum sensing toward biofilm formation under nonstress conditions, which is different from previous findings (22, 23). An inverse regulation between *adeG* and *adeJ* or *adeB* could be due to a fitness cost (58) during quorum sensing (Fig. 2). Moreover, typically as shown in Fig. 4, the strain HF28, which lacks the *abaR* gene (Fig. 1), exhibited a robust biofilm formation ability (RBFI = 7.57), while the strain HF32, which harbors a complete AbaI/AbaR system (Fig. 1), exhibited the lowest biofilm formation ability (RBFI = 0.51). In addition, an antibiotic-induced biofilm formation phenomenon was also observed in strains HF1, HF15, and HF51 (Fig. 5), all of which lack the *abaR* gene (Fig. 1). A deficiency in AbaI/AbaR quorum sensing was observed to be a common characteristic that was genetically displayed by IV and V type strains (Fig. 1; Table 2). These observations suggest that there are certain mechanisms other than AbaI/AbaR quorum sensing involved in the regulation of biofilm formation by *A. baumannii*. In addition, in view of the correlation of expression between *adeG* and *abaR*, it is also possible that AbaI/AbaR in turn regulates the expression of AdeFGH.

Synergistic antibiofilm effects of PB in combination with CAZ against *A. baumannii*. Typically, as shown in Fig. 5, the combined antibiofilm effects varied depending on the strains and the antibiotics used. Although the use of PB (1/8 × MIC,
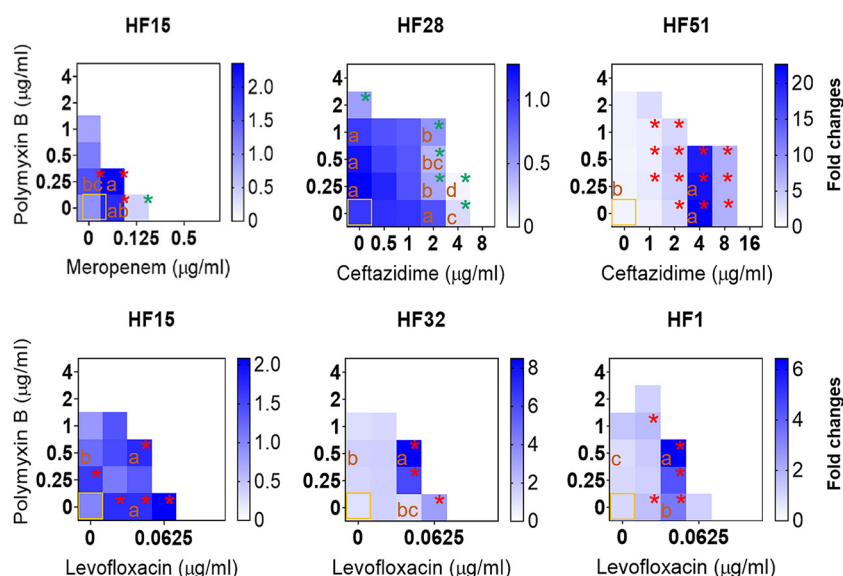
FIG 5 Heat map of antibiofilm effects of polymyxin B in combination with meropenem, levofloxacin, and ceftazidime against representative strains of *A. baumannii*. Boxes with orange borders refer to control without antibiotic treatment. All data are presented as means of three biological replicates. The significances were determined by nonparametric one-way ANOVA. Red asterisks indicate significant increases at a *P* value of 0.05 compared to control. Green asterisks indicate significant decreases at a *P* value of 0.05 compared to control. Boxes with different lowercase (a to d) within treatments are significantly different at *P* < 0.05.

0.25 μg/mL) and MEM (1/4 × MIC, 0.0625 μg/mL) alone significantly increased the biofilm formation ability of HF15, the combined use of PB and MEM did not synergistically induce the biofilm formation under this subinhibitory concentration condition. Similarly, although LEV alone significantly increased the biofilm formation ability of HF15, the combined use of PB and LEV did not synergistically induce the biofilm formation. However, the combined use of PB (1/4 × MIC, 0.5 μg/mL) and LEV (1/4 × MIC, 0.03125 μg/mL) synergistically (*P* < 0.05) induced the biofilm formation of HF32 and HF1 compared to the individual induction effect. Particularly for HF28, a strain naturally having a robust biofilm formation ability (Fig. 4), although PB in combination with CAZ has failed to achieve a synergistic inhibitory effect on the growth of planktonic cells, the combination with a wide range of concentration of PB (from 1/4 to 1/16 × MIC) and CAZ (from 1/2 to1/4 × MIC), in contrast, exhibited a synergy inhibitory effect on the biofilm formation of this strain (Fig. 5). Induction of biofilm formation by *A. baumannii* has been found to be associated with the AbaI/AbaR quorum sensing in response to antibiotics (22, 23). Whether the achievement of the synergistic antibiofilm effect is related to a deficiency of AbaI/AbaR quorum sensing is worthy of further study, because it could be important for further consideration of its combined effect with quorum quenching (59). In addition, the biofilm formation of HF51 was significantly enhanced under the condition of a series of subinhibitory concentrations of CAZ alone, but PB and CAZ did not have a significant inducing effect on the formation of biofilm under almost all combinations of different concentrations (Fig. 5). Overall, compared with LEV and MEM, PB in combination with CAZ could be a suitable choice in terms of antibiofilm applications.

In summary, our data support and extend the analysis of the correlation among antibiotic resistance, biofilm formation, and pathogenicity. Carbapenem-sensitive *A. baumannii* strains were demonstrated to be less pathogenic but stronger to form biofilm. The major finding of this study is that the combination of PB and CAZ displays a significant synergistic inhibitory effect against robust biofilm formed by certain genotypes of *A. baumannii* strains that are characterized by having deficiency in AbaI/AbaR quorum

sensing. This study provides a theoretical basis for clinical applications of polymyxin-based combination in antibiofilm therapy.

MATERIALS AND METHODS

Bacterial collection and identification. Bacterial samples were obtained from the First Affiliated Hospital of Anhui Medical University, a tertiary first-class hospital in China with 4,990 beds. A total of 103 *A. baumannii* strains were mainly collected from patients who were hospitalized in wards associated with intensive care unit (ICU), the respiratory and critical illness unit, and the burn unit from July to October 2020 (Table S1). The identification of these *A. baumannii* strains was performed with matrix-assisted laser desorption ionization-time of flight mass spectrometry (MALDI-TOF MS) on a Vitek MS system (bioMérieux, Marcy l'Étoile, France).

MIC determination assay. The susceptibilities to meropenem (MEM), levofloxacin (LEV), ceftazidime (CAZ), and polymyxin B (PB) of *A. baumannii* strains were tested in 103 *A. baumannii* strains according to a previously used broth microdilution method (22) with some modification. Briefly, culture medium with or without bacterial cells was served as positive and negative controls, respectively. The optical density (OD) of each well was determined at 600 nm in a BioTek Synergy2 microplate reader. The inhibition rate (%) was calculated as $[(OD_{positive\ control} - OD_{negative\ control}) - (OD_{treatment} - OD_{negative\ control})]/(OD_{positive\ control} - OD_{negative\ control}) \times 100\%$. The MIC was determined as the lowest concentration of antibiotic at which there was growth inhibition of $\geq 99\%$. The MIC values obtained by using cation-adjusted Mueller-Hinton (MH) medium and nutrient broth (NB) medium, respectively, were compared in 103 clinical strains and a type strain of *A. baumannii* ATCC 19606. The susceptibilities of at least three independent replicates were tested and interpreted according to CLSI guidelines.

Biofilm formation assay. The biofilm formation assays were performed according a previous method (22) with slight modification. Briefly, the biofilm remaining in each well was stained with a 0.1% crystal violet (CV) (Sigma) solution at 37°C for 10 min. The stained biofilm cells were destained with 95% ethanol and measured at 600 nm ($CV_{biofilm}$). The wells without inoculation were stained and used as the negative control ($CV_{control}$) to reduce the background staining from the CV-stained biofilm cells. The ability to form a biofilm was expressed using a biofilm formation index ($BFI = [CV_{biofilm} - CV_{control}]/OD_{planktonic}$). The type strain *A. baumannii* ATCC 19606 was used as a positive standard strain for biofilm formation to calculate the relative biofilm formation capacity ($RBFI = BFI_{isolate}/BFI_{A.\ baumannii\ ATCC\ 19606}$). The biofilm formation of at least three independent replicates for 103 clinic *A. baumannii* strains was tested.

Surface motility assay. Surface motility assay was carried out by using Luria-Bertani media (Difco) solidified with 0.5% agar in petri dishes. The dishes were point-inoculated from an active culture with a sterile iron wire and incubated at 37°C for 24 h. Swarming motility was assessed by measuring the circular turbid zones formed by the bacterial cells migrating away from the point of inoculation. The surface motility was detected in at least three independent replicates for 103 clinic *A. baumannii* strains.

Gene detection. A total of 103 *A. baumannii* strains were detected for the presence of genes, including RND efflux-associated *adeA*, *adeB*, *adeC*, *adeS*, *adeR*, *adeF*, *adeG*, *adeH*, *adeL*, *adeI*, *adeJ*, *adeK*, and *adeN*; quorum sensing-associated *abaI* and *abaR*; carbapenemase *bla*_{OXA-23}; and insertion sequence IS*Aba1* by PCR method with the specific primers showed in Table S2. DNA was extracted with QIAamp DNA blood kit (Qiagen, Valencia, CA). The amplification conditions were 94°C for 5 min; 35 cycles of 30 s at 94°C, 30 s at 56°C, and 2 min at 72°C; and a final extension of 7 min at 72°C. Amplicons were electrophoresed in gel agarose 1.5% containing 0.1% GoldView and visualized under gel documentation system with UV transilluminator (Bio-Rad). Each strain was detected in at least two independent replicates to confirm the presence of genes.

Molecular fingerprinting. The enterobacterial repetitive intergenic consensus (ERIC) sequence-based PCR fingerprinting assay was performed with a previously used method (22). Fingerprints were determined on the basis of at least three independent replicates of tests. A hierarchical cluster analysis was performed using the average linkage method described by Nei and Li (60). Cytoscape software was used to generate the network between genotypes and bacterial source.

Reverse Transcription-PCR assays. Transcriptional analysis was performed according to a previously used method (22) and with a minor modifications. Briefly, total RNA was extracted with the RNeasy Protect Bacteria minikit (Qiagen). cDNA was synthesized using a reverse transcription kit (Qiagen) in a 20-μl reaction system. The PCR amplification was performed using the ABI 7500 real-time PCR system (Applied Biosystems, Foster City, CA). Nine carbapenem-resistant strains and five carbapenem-sensitive strains were randomly chosen for transcriptional analysis. Each sample was run in triplicate. The comparative threshold cycle (C_T) method was used to analyze the relative expression of the targeted genes. The C_T value of the reference gene *rpoB* was used to calculate the ΔC_T.

Antimicrobial checkerboard assays for planktonic *A. baumannii*. Since the MIC value of highly resistant strains cannot be detected within the limited concentration range of antibiotics, drug-sensitive strains or low-resistant strains were considered for checkerboard assays. Finally, seven representative strains (four representative strains with I, III, IV, and VII type, respectively, and three representative strains including HF28 [the most robust strains in biofilm formation] with V type) were chosen to investigate the combined effects of antibiotics against strains with different genotypes. A broth microdilution checkerboard procedure (61) with a slight modification was used to determine the inhibitory effect of antibiotic combinations on the growth of planktonic cells of *A. baumannii* strains. Each drug was serially diluted at six concentrations to create an 6×6 matrix in a 96-well plate. Briefly, antibiotic A (PB) was diluted in wells along the abscissa on the left half of the plate, while antibiotic B (MEM, LEV, or CAZ) was diluted in wells along the ordinate on the right half of the plate. The dilutions of antibiotic B were then

parallelly transferred and mixed with antibiotic A at the left half plate correspondingly. After inoculation, the plates with a bacterial population of approximately 10^6 CFU/mL in final 200 μl of each well were incubated with at 37°C for 20 h. Each test was performed in three independent replicates. Absorbance at 600 nm of bacterial culture was collected after incubation. The fractional inhibitory concentration (FIC) was calculated for the first well with bacterial growth inhibition ≥99% in each row of the micro-plate containing all antimicrobial agents as follows: FIC of drug A (FIC_A) = MIC of drug A in combination/ MIC of drug A alone, and FIC of drug B (FIC_B) = MIC of drug B in combination/MIC of drug B alone. According to method described by Lewis et al. (62), the combined antimicrobial effect was evaluated by using a FIC index (FICI) = FIC_A + FIC_B and interpreted as synergy (FICI ≤ 0.5), additivity (0.5 < FICI < 1), indifference (1 ≤ FICI < 4), and antagonism (4 ≤ FICI). The FICs were confirmed based on three independent replicates of test.

Antibiofilm checkerboard assays. Five representative strains with FIC ≤ 1 in response to different antibiotic combinations were further tested to observe the combined effects of antibiotics on the biofilm formation. This assay was evaluated on the basis of the modified two-dimensional checkerboard method and the biofilm formation assay described above. Briefly, the well at the top right corner of the 6 × 6 matrix was chosen as the negative control to reduce the background staining from the CV-stained biofilm cells. Biofilm formed in the well at the bottom left corner of the matrix was used as the positive control to calculate the fold changes in biofilm formation. The biofilm having the most significant change in formation in the combination matrix was vertically and horizontally compared with that formed under conditions of exposure to the corresponding concentration of each single antibiotic. Synergistic effect in biofilm formation between two antibiotics was defined as a combined change in value that is statistically greater than the sum of the individual changes. The data were collected based on three independent replicates of tests.

Data analysis. The experimental data were analyzed using IBM SPSS Statistics 19. The chi-square test was used for the association of categorical variables, while Student's t test was used for the comparison of means and the correlation of variables used Spearman's correlation coefficient, with ρ between −1 and +1.

SUPPLEMENTAL MATERIAL

Supplemental material is available online only.

SUPPLEMENTAL FILE 1, PDF file, 0.8 MB.

ACKNOWLEDGMENTS

REFERENCES

1. Guerrero DM, Perez F, Conger NG, Solomkin JS, Adams MD, Rather PN, Bonomo RA. 2010. *Acinetobacter baumannii*-associated skin and soft tissue infections: recognizing a broadening spectrum of disease. Surg Infect 11:49–57. https://doi.org/10.1089/sur.2009.022.

2. Weinstein RA, Gaynes R, Edwards JR, National Nosocomial Infections Surveillance System. 2005. Overview of nosocomial infections caused by Gram-negative bacilli. Clin Infect Dis 41:848–854. https://doi.org/10.1086/432803.

3. Chaari A, Mnif B, Bahloul M, Mahjoubi F, Chtara K, Turki O, Gharbi N, Chelly H, Hammami A, Bouaziz M. 2013. *Acinetobacter baumannii* ventilator-associated pneumonia: epidemiology, clinical characteristics, and prognosis factors. Int J Infect Dis 17:e1225-8–e1228. https://doi.org/10.1016/j.ijid.2013.07.014.

4. Cisneros JM, Reyes MJ, Pachon J, Becerril B, Caballero FJ, Garcia-Garmendia JL, Ortiz C, Cobacho AR. 1996. Bacteremia due to *Acinetobacter baumannii*: epidemiology, clinical findings, and prognostic features. Clin Infect Dis 22:1026–1032. https://doi.org/10.1093/clinids/22.6.1026.

5. Russell DL, Uslan DZ, Rubin ZA, Grogan TR, Martin EM. 2018. Multidrug resistant *Acinetobacter baumannii*: a 15-year trend analysis. Infect Control Hosp Epidemiol 39:608–611. https://doi.org/10.1017/ice.2018.52.

6. Perez S, Innes GK, Walters MS, Mehr J, Arias J, Greeley R, Chew D. 2020. Increase in hospital-acquired carbapenem-resistant Acinetobacter baumannii infection and colonization in an acute care hospital during a surge in COVID-19 admissions – New Jersey, February–July 2020. MMWR Morb Mortal Wkly Rep 69:1827–1831. https://doi.org/10.15585/mmwr.mm6948e1.

7. Evans BA, Hamouda A, Amyes SG. 2013. The rise of carbapenem-resistant *Acinetobacter baumannii*. Curr Pharm Des 19:223–238. https://doi.org/10.2174/138161213804070285.

8. Liu B, Liu L. 2021. Molecular epidemiology and mechanisms of carbapenem-resistant *Acinetobacter baumannii* isolates from ICU and respiratory department patients of a Chinese university hospital. Infect Drug Resist 14:743–755. https://doi.org/10.2147/IDR.S299540.

9. Jacobs AC, Thompson MG, Black CC, Kessler JL, Clark LP, McQueary CN, Gancz HY, Corey BW, Moon JK, Si Y, Owen MT, Hallock JD, Kwak YI, Summers A, Li CZ, Rasko DA, Penwell WF, Honnold CL, Wise MC, Waterman PE, Lesho EP, Stewart RL, Actis LA, Palys TJ, Craft DW, Zurawski DV. 2014. AB5075, a highly virulent isolate of *Acinetobacter baumannii*, as a model strain for the evaluation of pathogenesis and antimicrobial treatments. mBio 5:e01076-14–e01014. https://doi.org/10.1128/mBio.01076-14.

10. Li J, Yu T, Luo Y, Peng JY, Li YJ, Tao XY, Hu YM, Wang HC, Zou MX. 2020. Characterization of carbapenem-resistant hypervirulent *Acinetobacter baumannii* strains isolated from hospitalized patients in the mid-south region of China. BMC Microbiol 20:281. https://doi.org/10.1186/s12866-020-01957-7.

11. Da Silva GJ, Domingues S. 2017. Interplay between colistin resistance, virulence and fitness in *Acinetobacter baumannii*. Antibiotics 6:28. https://doi.org/10.3390/antibiotics6040028.

12. Hazhirkamal M, Zarei O, Movahedi M, Karami P, Shokoohizadeh L, Taheri M. 2021. Molecular typing, biofilm production, and detection of carbapenemase genes in multidrug-resistant *Acinetobacter baumannii* isolated from different infection sites using ERIC-PCR in Hamadan, west of Iran. BMC Pharmacol Toxicol 22:32. https://doi.org/10.1186/s40360-021-00504-y.

13. Hawkey J, Ascher DB, Judd LM, Wick RR, Kostoulias X, Cleland H, Spelman DW, Padiglione A, Peleg AY, Holt KE. 2018. Evolution of carbapenem resistance in *Acinetobacter baumannii* during a prolonged infection. Microb Genom 4:e000165.

14. Hamidian M, Nigro SJ. 2019. Emergence, molecular mechanisms and global spread of carbapenem-resistant *Acinetobacter baumannii*. Microb Genom 5:e000306.

15. Turton JF, Ward ME, Woodford N, Kaufmann ME, Pike R, Livermore DM, Pitt TL. 2006. The role of IS*Aba1* in expression of OXA carbapenemase genes in *Acinetobacter baumannii*. FEMS Microbiol Lett 258:72–77. https://doi.org/10.1111/j.1574-6968.2006.00195.x.

16. Zhu LJ, Pan Y, Gao CY, Hou PF. 2020. Distribution of carbapenemases and efflux pump in carbapenem-resistance *Acinetobacter baumannii*. Ann Clin Lab Sci 50:241–246.

17. Amala Reena A, Subramaniyan A, Kanungo R. 2017. Biofilm formation as a virulence factor of *Acinetobacter baumannii*: an emerging pathogen in critical care units. J Curr Res Sci Med 3:74–78. https://doi.org/10.4103/jcrsm.jcrsm_66_17.

18. Clemmer KM, Bonomo RA, Rather PN. 2011. Genetic analysis of surface motility in *Acinetobacter baumannii*. Microbiology 157:2534–2544. https://doi.org/10.1099/mic.0.049791-0.

19. Oh MH, Han K. 2020. AbaR is a LuxR type regulator essential for motility and the formation of biofilm and pellicle in *Acinetobacter baumannii*. Genes Genomics 42:1339–1346. https://doi.org/10.1007/s13258-020-01005-8.

20. Dou Y, Song F, Guo F, Zhou Z, Zhu C, Xiang J, Huan J. 2017. *Acinetobacter baumannii* quorum-sensing signalling molecule induces the expression of drug-resistance genes. Mol Med Rep 15:4061–4068. https://doi.org/10.3892/mmr.2017.6528.

21. Nicol M, Alexandre S, Luizet JB, Skogman M, Jouenne T, Salcedo SP, Dé E. 2018. Unsaturated fatty acids affect quorum sensing communication system and inhibit motility and Biofilm formation of *Acinetobacter baumannii*. Int J Mol Sci 19:214. https://doi.org/10.3390/ijms19010214.

22. He X, Lu F, Yuan F, Jiang D, Zhao P, Zhu J, Cheng H, Cao J, Lu G. 2015. Biofilm formation caused by clinical *Acinetobacter baumannii* isolates is associated with overexpression of the AdeFGH efflux pump. Antimicrob Agents Chemother 59:4817–4825. https://doi.org/10.1128/AAC.00877-15.

23. Navidifar T, Amin M, Rashno M. 2019. Effects of sub-inhibitory concentrations of meropenem and tigecycline on the expression of genes regulating pili, efflux pumps and virulence factors involved in biofilm formation by *Acinetobacter baumannii*. Infect Drug Resist 12:1099–1111. https://doi.org/10.2147/IDR.S199993.

24. Bergen PJ, Smith NM, Bedard TB, Bulman ZP, Cha R, Tsuji BT. 2019. Rational combinations of polymyxins with other antibiotics, p 251–288. *In* Li J, Nation RL, Kaye KS (ed), Polymyxin antibiotics: from laboratory bench to bedside. Springer International Publishing, Cham, Switzerland.

25. Aljindan R, Alsamman K, Elhadi N. 2018. ERIC-PCR genotyping of *Acinetobacter baumannii* isolated from different clinical specimens. Saudi J Med Sci 6:13–17. https://doi.org/10.4103/sjmms.sjmms_138_16.

26. Hu F, Guo Y, Zhu D, Wang F, Jiang X, Xu Y, Zhang X, Zhang Z, Ji P, Xie Y, Kang M, Wang C, Wang A. 2020. CHINET surveillance of bacterial resistance across tertiary hospitals in 2019. Chin J Infect Chemother 20:233–243.

27. Lima WG, Brito JCM, Cardoso BG, Cardoso VN, de Paiva MC, de Lima ME, Fernandes SOA. 2020. Rate of polymyxin resistance among *Acinetobacter baumannii* recovered from hospitalized patients: a systematic review and meta-analysis. Eur J Clin Microbiol Infect Dis 39:1427–1438. https://doi.org/10.1007/s10096-020-03876-x.

28. Mak JK, Kim MJ, Pham J, Tapsall J, White PA. 2009. Antibiotic resistance determinants in nosocomial strains of multidrug-resistant *Acinetobacter baumannii*. J Antimicrob Chemother 63:47–54. https://doi.org/10.1093/jac/dkn454.

29. Fournier PE, Vallenet D, Barbe V, Audic S, Ogata H, Poirel L, Richet H, Robert C, Mangenot S, Abergel C, Nordmann P, Weissenbach J, Raoult D, Claverie JM. 2006. Comparative genomics of multidrug resistance in *Acinetobacter baumannii*. PLoS Genet 2:e7. https://doi.org/10.1371/journal.pgen.0020007.

30. Lima WG, Alves MC, Cruz WS, Paiva MC. 2018. Chromosomally encoded and plasmid-mediated polymyxins resistance in *Acinetobacter baumannii*: a huge public health threat. Eur J Clin Microbiol Infect Dis 37:1009–1019. https://doi.org/10.1007/s10096-018-3223-9.

31. Elabd FM, Al-Ayed MS, Asaad AM, Alsareii SA, Qureshi MA, Musa HA. 2015. Molecular characterization of oxacillinases among carbapenem-resistant *Acinetobacter baumannii* nosocomial isolates in a Saudi hospital. J Infect Public Health 8:242–247. https://doi.org/10.1016/j.jiph.2014.10.002.

32. Mugnier PD, Poirel L, Nordmann P. 2009. Functional analysis of insertion sequence IS*Aba1*, responsible for genomic plasticity of *Acinetobacter baumannii*. J Bacteriol 191:2414–2418. https://doi.org/10.1128/JB.01258-08.

33. Zhang L, Murphy PJ, Kerr A, Tate ME. 1993. *Agrobacterium* conjugation and gene regulation by *N*-acyl-L-homoserine lactones. Nature 362:446–448. https://doi.org/10.1038/362446a0.

34. Lu Y, Zeng J, Wu B, Shunmei E, Wang L, Cai R, Zhang N, Li Y, Huang X, Huang B, Chen C. 2017. Quorum sensing *N*-acyl homoserine lactones-SdiA suppresses *Escherichia coli-Pseudomonas aeruginosa* conjugation through inhibiting traI expression. Front Cell Infect Microbiol 7:7.

35. Lee Y, Kim YR, Kim J, Park YJ, Song W, Shin JH, Uh Y, Lee K, Lee SH, Cho JH, Yong D, Jeong SH, Lee K, Chong Y. 2013. Increasing prevalence of *bla*OXA-23-carrying *Acinetobacter baumannii* and the emergence of *bla*OXA-182-carrying *Acinetobacter nosocomialis* in Korea. Diagn Microbiol Infect Dis 77:160–163. https://doi.org/10.1016/j.diagmicrobio.2013.06.009.

36. Chen TL, Lee YT, Kuo SC, Hsueh PR, Chang FY, Siu LK, Ko WC, Fung CP. 2010. Emergence and distribution of plasmids bearing the *bla*OXA-51-like gene with an upstream IS*Aba1* in carbapenem-resistant *Acinetobacter baumannii* isolates in Taiwan. Antimicrob Agents Chemother 54:4575–4581. https://doi.org/10.1128/AAC.00764-10.

37. Coyne S, Courvalin P, Perichon B. 2011. Efflux-mediated antibiotic resistance in *Acinetobacter* spp. Antimicrob Agents Chemother 55:947–953. https://doi.org/10.1128/AAC.01388-10.

38. Hoang Quoc C, Nguyen Thi Phuong T, Nguyen Duc H, Tran Le T, Tran Thi Thu H, Nguyen Tuan S, Phan Trong L. 2019. Carbapenemase genes and multidrug resistance of *Acinetobacter baumannii*: a cross sectional study of patients with pneumonia in southern Vietnam. Antibiotics 8:148. https://doi.org/10.3390/antibiotics8030148.

39. Sun JR, Perng CL, Chan MC, Morita Y, Lin JC, Su CM, Wang WY, Chang TY, Chiueh TS. 2012. A truncated AdeS kinase protein generated by IS*Aba1* insertion correlates with tigecycline resistance in *Acinetobacter baumannii*. PLoS One 7:e49534. https://doi.org/10.1371/journal.pone.0049534.

40. Marchand I, Damier-Piolle L, Courvalin P, Lambert T. 2004. Expression of the RND-type efflux pump AdeABC in *Acinetobacter baumannii* is regulated by the AdeRS two-component system. Antimicrob Agents Chemother 48:3298–3304. https://doi.org/10.1128/AAC.48.9.3298-3304.2004.

41. Coyne S, Rosenfeld N, Lambert T, Courvalin P, Perichon B. 2010. Overexpression of resistance-nodulation-cell division pump AdeFGH confers multidrug resistance in *Acinetobacter baumannii*. Antimicrob Agents Chemother 54:4389–4393. https://doi.org/10.1128/AAC.00155-10.

42. Rosenfeld N, Bouchier C, Courvalin P, Perichon B. 2012. Expression of the resistance-nodulation-cell division pump AdeIJK in *Acinetobacter baumannii* is regulated by AdeN, a TetR-type regulator. Antimicrob Agents Chemother 56:2504–2510. https://doi.org/10.1128/AAC.06422-11.

43. Ruzin A, Keeney D, Bradford PA. 2007. AdeABC multidrug efflux pump is associated with decreased susceptibility to tigecycline in *Acinetobacter calcoaceticus-Acinetobacter baumannii* complex. J Antimicrob Chemother 59:1001–1004. https://doi.org/10.1093/jac/dkm058.

44. Saranathan R, Pagal S, Sawant AR, Tomar A, Madhangi M, Sah S, Satti A, Arunkumar KP, Prashanth K. 2017. Disruption of *tetR* type regulator *adeN* by mobile genetic element confers elevated virulence in *Acinetobacter baumannii*. Virulence 8:1316–1334. https://doi.org/10.1080/21505594.2017.1322240.

45. Rodriguez-Bano J, Marti S, Soto S, Fernandez-Cuenca F, Cisneros JM, Pachon J, Pascual A, Martinez-Martinez L, McQueary C, Actis LA, Vila J, Spanish Group for the Study of Nosocomial Infections (GEIH). 2008. Biofilm formation in *Acinetobacter baumannii*: associated features and clinical implications. Clin Microbiol Infect 14:276–278. https://doi.org/10.1111/j.1469-0691.2007.01916.x.

46. Eijkelkamp BA, Stroeher UH, Hassan KA, Papadimitrious MS, Paulsen IT, Brown MH. 2011. Adherence and motility characteristics of clinical *Acinetobacter baumannii* isolates. FEMS Microbiol Lett 323:44–51. https://doi.org/10.1111/j.1574-6968.2011.02362.x.

47. Duan Q, Zhou M, Zhu L, Zhu G. 2013. Flagella and bacterial pathogenicity. J Basic Microbiol 53:1–8. https://doi.org/10.1002/jobm.201100335.

48. Mu X, Wang N, Li X, Shi K, Zhou Z, Yu Y, Hua X. 2016. The effect of colistin resistance-associated mutations on the fitness of *Acinetobacter baumannii*. Front Microbiol 7:1715. https://doi.org/10.3389/fmicb.2016.01715.

49. Smani Y, Lopez-Rojas R, Dominguez-Herrera J, Docobo-Perez F, Marti S, Vila J, Pachon J. 2012. *In vitro* and *in vivo* reduced fitness and virulence in ciprofloxacin-resistant *Acinetobacter baumannii*. Clin Microbiol Infect 18: E1–4. https://doi.org/10.1111/j.1469-0691.2011.03695.x.

50. Taguchi F, Suzuki T, Inagaki Y, Toyoda K, Shiraishi T, Ichinose Y. 2010. The siderophore pyoverdine of *Pseudomonas syringae* pv. tabaci 6605 is an intrinsic virulence factor in host tobacco infection. J Bacteriol 192: 117–126. https://doi.org/10.1128/JB.00689-09.

51. Ko KS, Suh JY, Kwon KT, Jung SI, Park KH, Kang CI, Chung DR, Peck KR, Song JH. 2007. High rates of resistance to colistin and polymyxin B in subgroups of *Acinetobacter baumannii* isolates from Korea. J Antimicrob Chemother 60:1163–1167. https://doi.org/10.1093/jac/dkm305.

52. Carrasco LDM, Dabul ANG, Boralli C, Righetto GM, Carvalho ISE, Dornelas JV, Martins da Mata CPS, de Araujo CA, Leite EMM, Lincopan N, Camargo I. 2021. Polymyxin resistance among XDR ST1 carbapenem-resistant *Acinetobacter baumannii* clone expanding in a teaching hospital. Front Microbiol 12:622704. https://doi.org/10.3389/fmicb.2021.622704.

53. Falagas ME, Kasiakou SK. 2005. Colistin: the revival of polymyxins for the management of multidrug-resistant Gram-negative bacterial infections. Clin Infect Dis 40:1333–1341. https://doi.org/10.1086/429323.

54. Paul M, Leibovici L. 2009. Combination antimicrobial treatment versus monotherapy: the contribution of meta-analyses. Infect Dis Clin North Am 23:277–293. https://doi.org/10.1016/j.idc.2009.01.004.

55. Alav I, Sutton JM, Rahman KM. 2018. Role of bacterial efflux pumps in biofilm formation. J Antimicrob Chemother 73:2003–2020. https://doi.org/10.1093/jac/dky042.

56. Niu C, Clemmer KM, Bonomo RA, Rather PN. 2008. Isolation and characterization of an autoinducer synthase from *Acinetobacter baumannii*. J Bacteriol 190:3386–3392. https://doi.org/10.1128/JB.01929-07.

57. Stacy DM, Welsh MA, Rather PN, Blackwell HE. 2012. Attenuation of quorum sensing in the pathogen *Acinetobacter baumannii* using non-native N-Acyl homoserine lactones. ACS Chem Biol 7:1719–1728. https://doi.org/10.1021/cb300351x.

58. Yoon EJ, Balloy V, Fiette L, Chignard M, Courvalin P, Grillot-Courvalin C. 2016. Contribution of the Ade resistance-nodulation-cell division-type efflux pumps to fitness and pathogenesis of *Acinetobacter baumannii*. mBio 7:e00697-16. https://doi.org/10.1128/mBio.00697-16.

59. Zhong S, He S. 2021. Quorum sensing inhibition or quenching in *Acinetobacter baumannii*: the novel therapeutic strategies for new drug development. Front Microbiol 12:558003. https://doi.org/10.3389/fmicb.2021.558003.

60. Nei M, Li WH. 1979. Mathematical model for studying genetic variation in terms of restriction endonucleases. Proc Natl Acad Sci U S A 76: 5269–5273. https://doi.org/10.1073/pnas.76.10.5269.

61. MacNair CR, Stokes JM, Carfrae LA, Fiebig-Comyn AA, Coombes BK, Mulvey MR, Brown ED. 2018. Overcoming mcr-1 mediated colistin resistance with colistin in combination with other antibiotics. Nat Commun 9: 458. https://doi.org/10.1038/s41467-018-02875-z.

62. Lewis RE, Diekema DJ, Messer SA, Pfaller MA, Klepser ME. 2002. Comparison of Etest, chequerboard dilution and time-kill studies for the detection of synergy or antagonism between antifungal agents tested against *Candida* species. J Antimicrob Chemother 49:345–351. https://doi.org/10.1093/jac/49.2.345.